

# Computer Simulation of PEO/Layered-Silicate Nanocomposites: 2. Lithium Dynamics in PEO/Li<sup>+</sup> Montmorillonite Intercalates

V. Kuppa and E. Manias\*

Department of Materials Science and Engineering, The Pennsylvania State University,  
325-D Steidle Building, University Park, Pennsylvania 16802

Received November 13, 2001. Revised Manuscript Received February 6, 2002

Molecular dynamics simulations are used to explore poly(ethylene oxide)/Li<sup>+</sup> complexes, comparing bulk and nanoscopically confined systems. We focus on lithium ion dynamics, so as to elucidate the molecular mechanisms of ionic motion in these two environments. The confined systems mimic 0.8 nm thin intercalates between mica-type layers (montmorillonite). Simulations of the Li<sup>+</sup>/bulk PEO system show a clear change in the ion transport mechanism from a hopping fashion, at low temperatures, to a random Brownian-like diffusion, at higher temperatures. In sharp contrast, the intercalated, nanoconfined, systems display a single hopping mechanism throughout the same temperature range, dictated by the unique nature of the lithium coordination to the mica-type surfaces and the confined PEO.

## Introduction

The past few years have seen an increased interest in organic/inorganic “hybrid” materials, as model systems to study confined polymers. One of the most actively explored classes of such materials is that of polymers intercalated between mica-type, inorganic layers.<sup>1</sup> Where a polymer-electrolyte/cation system is confined between inorganic layers,<sup>2–7</sup> these materials exhibit interesting electrical and mechanical responses, rendering them promising candidates for applications as electrolytes in all solid-state batteries.<sup>7</sup> In these systems, poly(ethylene oxide) (PEO) is confined in well-defined 0.8 nm wide slits, formed by self-assembly of parallelly stacked, negatively charged, montmorillonite (MMT) layers, which are 0.97 nm thin and about 0.5 μm in lateral dimensions.

A variety of techniques, including solid-state NMR<sup>6</sup> and conductivity studies,<sup>7</sup> have been employed to probe the Li<sup>+</sup> dynamics in these severe confinements, and a very striking picture is emerging on the behavior of Li<sup>+</sup> in nanometer-thin slit pores filled with PEO<sup>6,7,8</sup>. Namely, (a) the temperature dependence of the Li<sup>+</sup> dynamics in the intercalated, nanoscopically confined, systems does not show a change near the PEO melting point.<sup>6,7</sup>

Moreover, (b) conductivity studies at room/low temperature reveal an unexpectedly faster motion for Li<sup>+</sup> in this severe confinement, compared to Li<sup>+</sup> motion in the respective bulk systems. Several possible scenarios were proposed in the experimental studies<sup>6,7</sup> to account for these counterintuitive findings; however, these experiments cannot directly provide the relevant atomistic mechanisms; thus, a clear atomistic picture has yet to be developed.

Expanding on our previous study, where molecular modeling was used to investigate the structure of these systems,<sup>9</sup> we have performed molecular dynamics computer simulations especially focusing on the Li<sup>+</sup> dynamics. Our aim is to trace the mechanisms of Li<sup>+</sup> motion and to develop an atomistic understanding of the system dynamics, which can provide insight into the macroscopically observed behavior.

## Molecular Dynamics Simulation Details

Fully atomistic molecular dynamics simulations have been carried out in LiI/bulk PEO and PEO/Li<sup>+</sup> MMT intercalated systems. Two different force fields developed in earlier simulations of Li<sup>+</sup>/bulk PEO by Muller-Plathe<sup>10</sup> and Smith et al.<sup>11</sup> were also evaluated in our confined geometries, where the interactions with the montmorillonite sheets were modeled after Hackett et al.<sup>9</sup> Both sets of parameters reproduce well the structural PEO details of the confined systems as observed experimentally. However, the force field from ref 11 employed in the intercalated systems results in Li<sup>+</sup> and PEO segmental dynamics that mimic better the spin lattice relaxation NMR experiments.<sup>8</sup>

\* To whom correspondence should be addressed. E-mail: manias@psu.edu.

(1) Giannelis, E. P.; Krishnamoorti, R. K.; Manias, E. *Adv. Polym. Sci.* **1999**, *138*, 107.

(2) Wu, J.; Lerner, M. M. *Chem. Mater.* **1993**, *5*, 835.

(3) Vaia, R. A.; Sauer, B. B.; Tse, O. K.; Giannelis, E. P. *J. Polym. Sci. Polym. Phys.* **1997**, *35*, 59.

(4) Aranda, P.; Ruiz-Hutsky, E. *Chem. Mater.* **1992**, *4*, 1395.

(5) Wang, L.; Rocci-Lane, M.; Brazis, P.; Kannewurf, C. R.; Kim, Y.; Lee, W.; Choy, J.; Kanatzidis, M. G. *J. Am. Chem. Soc.* **2000**, *122*, 6629.

(6) Wong, S.; Vaia, R. A.; Giannelis, E. P.; Zax, D. B. *Solid State Ionics.* **1996**, *86*, 547.

(7) Vaia, R. A.; Vasudevan, S.; Krawiec, W.; Giannelis, E. P. *Adv. Mater.* **1995**, *7*, 154.

(8) Yang, D. K.; Zax, D. B. *J. Chem. Phys.* **1999**, *110*, 5325.

(9) Hackett, E.; Manias, E.; Giannelis, E. P. *Chem. Mater.* **2000**, *12*, 2161.

(10) Muller-Plathe, F.; *Acta Polymer.* **1994**, *45*, 259.

(11) Smith, G. D.; Jaffe, R. L.; Yoon, D. Y. *J. Phys. Chem.* **1993**, *97*, 12752; *J. Am. Chem. Soc.* **1995**, *117*, 530.

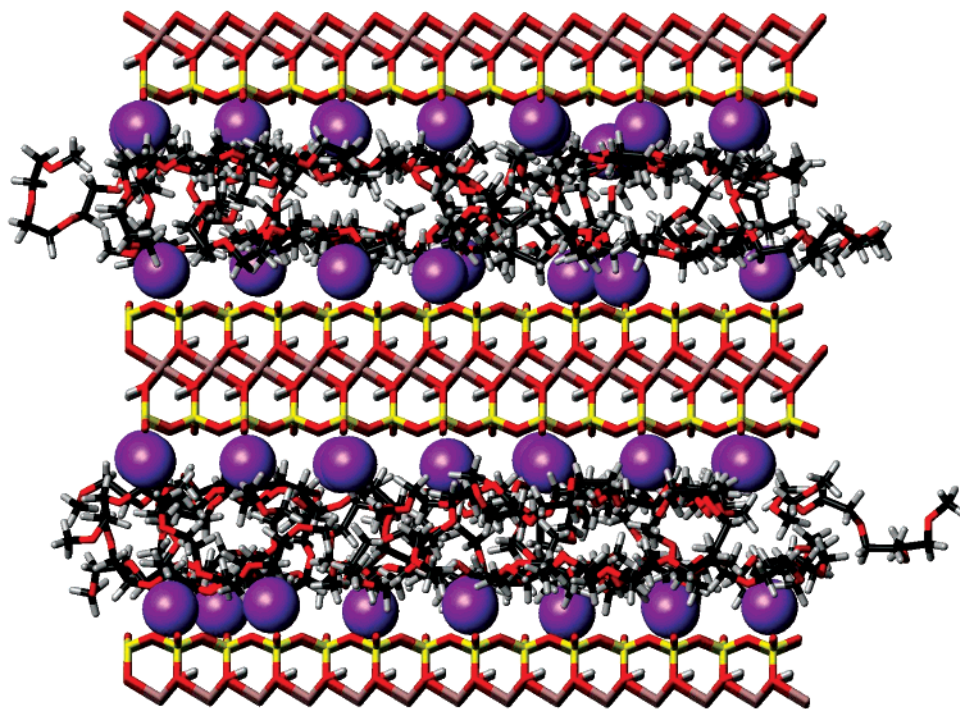


**Figure 1.** Schematic of a simulation box with double slit geometry. The PEO and the MMT layers are in a “stick” representation (O, red; C, black; Si, yellow; Al, light-purple), and the Li<sup>+</sup> are shown by their van der Waals spheres (purple spheres) for clarity.

For the bulk, constant NPT simulations were performed, paralleling those described in ref 11, with a cutoff radius of 0.9 nm and a distance-dependent dielectric constant.<sup>12</sup> The bulk systems consist of eight Li<sup>+</sup>I<sup>-</sup> units solvated by 69 PEO hexamers. The initial box size was varied, so as to match the PEO density to the experimental data<sup>13</sup> at each temperature. Subsequently, P and T were stabilized by a weak coupling to their reference values, via the Berendsen method.<sup>14</sup> Although our PEO chains are too small to form extended polymer crystals (spherulites), crystal regions do manifest themselves in our bulk PEO systems. Both the chain packing (quantified through the interchain C–C radial distribution function) and the chain conformations (helical *ttgttgg* sequences) are characteristic of a PEO crystalline structure at low *T*.<sup>15</sup> Moreover, when *T* is increased, these quantities satisfy the Lindemann criterion of melting just before 323 K; that is, crystal regions undergo a “melting” transition toward an amorphous structure in the neighborhood of 323 K. To quantify the extent of such crystalline regions in our simulations, we enumerate the crystalline dihedral *ttgttgg* hexads and *ttgttgg* enneads along the backbones of our chains, and also measured their melting with increasing *T*. For the bulk simulations, all densities (controlled by our isobaric NPT scheme) are consistent with the experimental density values (for semicrystalline and amorphous PEO).<sup>13</sup>

The confined systems were simulated at constant NVT, at four different temperatures. Periodic boundary

conditions were employed in all three directions, and a box size of 3.696 × 3.656 × 3.558 nm was used, which corresponds to two PEO/Li<sup>+</sup> films intercalated between two inorganic layers, as shown in Figure 1. This double slit geometry of PEO/Li<sup>+</sup> MMT was chosen as it allows for more accurate evaluation of the long-range electrostatic forces.<sup>16</sup> Long range corrections in the electrostatics were included through the generalized reaction field method<sup>17</sup> with an effective dielectric constant of 3.0 beyond 1.0 nm. The confined films are 0.8 nm thin and consist of 23 PEO hexamers and 21 Li<sup>+</sup> per MMT; both the film thickness as well as the PEO and Li<sup>+</sup> numbers were chosen to agree with the experimental values.<sup>6</sup> The time step in all simulations was 10<sup>-6</sup> ns. For each temperature, initial system configurations were taken from previous studies,<sup>9</sup> and after energy minimization and an equilibration MD run of 10 ns, productive runs of 2–10 ns were recorded, depending on *T*.

## Results and Discussion

Our aim here is to unveil the fundamental processes underlying the ionic motion and dynamics in the dry intercalated systems. Expanding upon previous work on the structure of intercalated PEO oligomers,<sup>9</sup> we performed MD simulations to contrast the Li<sup>+</sup> dynamics in bulk and nanoconfined PEO. To this end, we comparatively studied intercalated and bulk systems over a broad temperature range, as also explored experimentally.<sup>6</sup> The diffusion coefficients of lithium versus temperature, in the absence of an electric field, are shown

(12) Londano, J. D.; Annis, B. K.; Habenschuss, A.; Borodin, O.; Smith, G. D.; Turner, J. Z.; Soper, A. K. *Macromolecules* **1997**, *30*, 7151.

(13) Smith, G. D.; Yoon, D. Y.; Jaffe, R. L.; Colby, R. H.; Krishnamoorti, R.; Fetters, L. J. *Macromolecules* **1996**, *29*, 3462.

(14) Berendsen, H. J. C.; Postma, J. P. M.; van Gunsteren, W. F.; DiNola, A.; Haak, J. R. *J. Chem. Phys.* **1984**, *81*, 3684.

(15) Borodin, O.; Smith, G. S. *Macromolecules* **1998**, *31*, 8396.

(16) Chávez-Páez, M.; Van Workum, K.; de Pablo, L.; de Pablo, J. *J. Chem. Phys.* **2001**, *114*, 1405.

(17) Torini, I. G.; Sperb, R.; Smith, P. E.; van Gunsteren, W. F. *J. Chem. Phys.* **1995**, *102*, 5451.

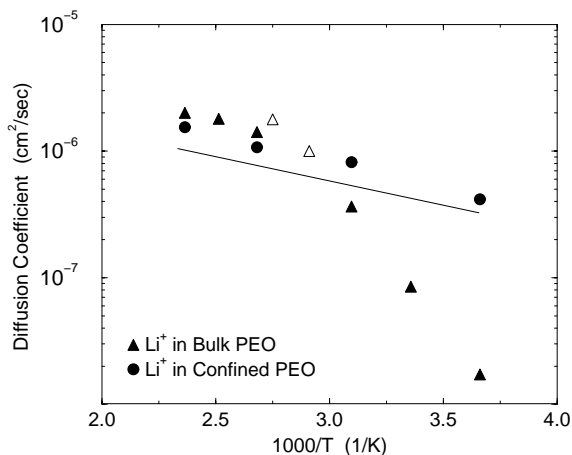


**Figure 2.** Temperature dependence of Li<sup>+</sup> diffusivities in bulk PEO and in 0.8 nm thin films of PEO, confined, intercalated, between MMT inorganic layers. The solid symbols are the diffusivities of these simulations, and the open symbols are from experiments ( $\Delta$  Li<sup>+</sup> in bulk PEO from ref 19). The solid line denotes the activation energy from conductivity measurements in intercalated systems<sup>7</sup> converted to diffusivities in the limit of zero electric field.

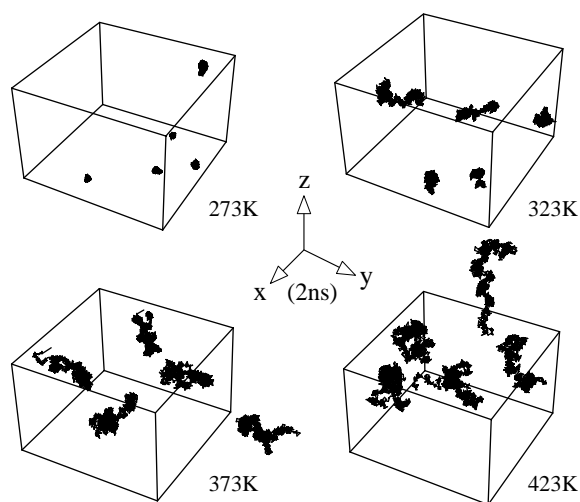


**Figure 3.** Typical Li<sup>+</sup> trajectories in bulk PEO over 2 ns, for various temperatures.

in Figure 2. The Arrhenius plot of Li<sup>+</sup> diffusivities shows two different slopes for the bulk system, at the higher and lower temperatures, whereas the confined system exhibits only a single VTF-like dependence. This behavior is strongly reminiscent of the experimental AC conductivity measurements<sup>7</sup> (the diffusion coefficients of Figure 2 are actually a measure of the “dark current” of those systems). Such a behavior suggests that there are two mechanisms of Li<sup>+</sup> motion in bulk PEO, above and below 330 K, whereas in the confined systems, a single mechanism seems to be in place throughout the studied temperature range.

In MD simulations, the mechanism of motion can be directly viewed by following the time trajectory of the particles. In Figure 3, we show the trajectory of a few representative Li<sup>+</sup> in bulk PEO, at various system temperatures. There is a clear change in the mechanism of lithium motion from the “hopping” fashion at lower temperatures to a random, almost Brownian-like, mo-

tion at higher temperatures. This behavior has been observed before<sup>18</sup> and is attributed to the balance between thermal energy of Li<sup>+</sup> and coordination energy of Li<sup>+</sup> and PEO monomers. Li<sup>+</sup> ions vibrate around mean positions defined by the complexing PEO chains, in a crown-like structure. Dihedral relaxations of these adjacent PEO units provide transient channels for lithium motion to nearby sites. As a consequence, at temperatures below  $T_m$ , where the polymer relaxations are inhibited, Li<sup>+</sup> ions are almost immobile (273 K). As the temperature increases, the polymer undergoes increasingly more configurational changes, which lead to more pathways for Li<sup>+</sup> motion. Coupled with the higher thermal energy that the Li<sup>+</sup> ions now possess, there exists less complexation with the PEO, resulting in an almost random nature of motion (423 K). The hopping mechanism, prevalent below the melting point, is conspicuous by its absence in these conditions.

In sharp contrast to the behavior seen in bulk PEO, the trajectories of the nanoscopically confined Li<sup>+</sup>/PEO systems show little change in the transport mechanism of the ions, over the same broad temperature range (Figure 4). Unlike Li<sup>+</sup> in bulk PEO, the confined system exhibits only quantitative changes with temperature, whereas the Li<sup>+</sup> motion follows a hopping mechanism throughout all of the temperatures studied. Moreover, the Li<sup>+</sup> are now coordinated to the MMT surfaces and much less to the confined PEO, as expected from the large negative charge of the MMT layers.<sup>9</sup> This is due to the mica-type cleavage plane of the MMT, which includes electrostatic energy minima positions defined by the surface oxygens. Although this strong Li<sup>+</sup>/MMT coordination is to be expected, the trajectories of the lithium cations on top of the inorganic confining surface are largely dictated by the PEO local motions. Namely, analysis of  $yz$  motion of the Li<sup>+</sup> ions shows clear evidence that the hopping mechanism of Li<sup>+</sup>, jumping from one local energy minimum on the MMT surface to another, is always through the proximal PEO units in the interlayer gallery (Figure 5). At all temperatures, thermal excitations cause the Li<sup>+</sup> to move slightly out of the MMT “pockets” and become coordinated to the PEO moieties present in the gallery. This new position is only momentarily stable as the lithium seeks to lower its potential energy by jumping back to the wall surface, oftentimes in a neighboring low energy pocket on the surface (Figure 5). Local motion of the proximal ethylene-oxide segments can mediate motion away from the original MMT “pocket”, thus enabling transport on top of the wall. Very often, when the proximal PEO does not undergo any segmental motion, the Li<sup>+</sup> moves back to the same position where it initially resided. A series of events of this progression account for most of the Li<sup>+</sup> trajectories recorded during the course of the entire run (Figure 4). Less often, a Li<sup>+</sup> moves further away from the MMT surface, toward the center of the confined PEO layer, and coordinated to the PEO segments, it can travel further away than the first-neighboring minimum energy pocket on the MMT surface. Such Li<sup>+</sup> motions occur for all temperatures studied and correspond to the infrequent longer walks seen in the  $xy$  projection of Figure 4.

(18) Muller-Plathe, F.; van Gunsteren, W. F. *J. Chem. Phys.* **1995**, *103*, 4745.

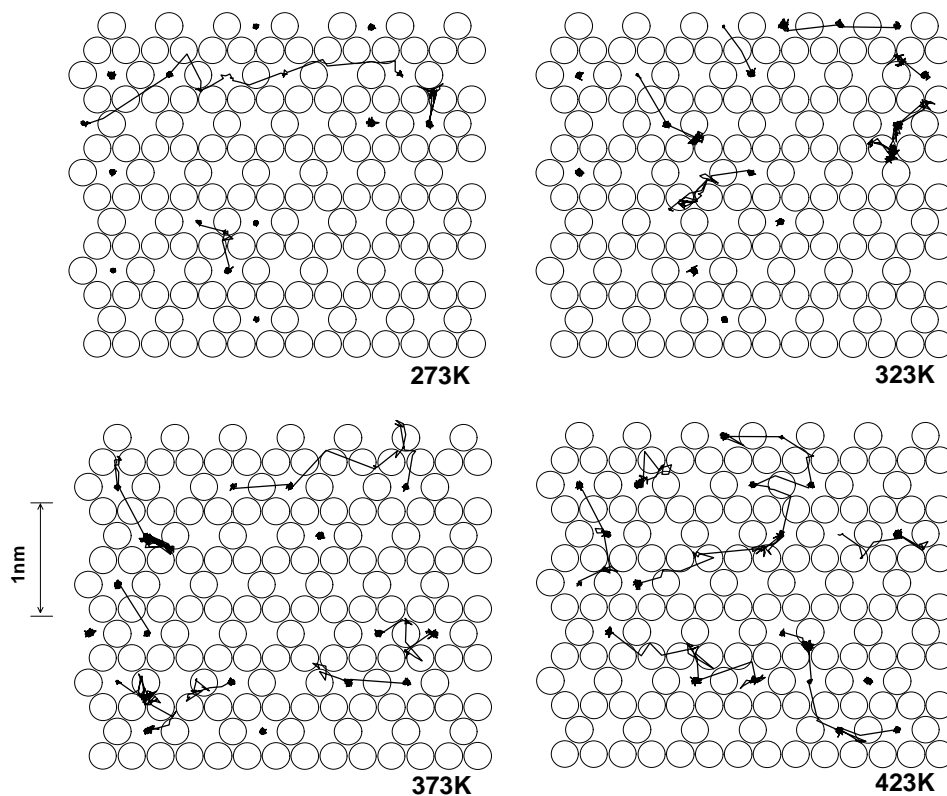


**Figure 4.**  $\text{Li}^+$  trajectories in confinement. The projection of few representative  $\text{Li}^+$  are shown on top of the  $xy$  MMT plane, over 5 ns and for various  $T$ . The surface oxygens of the MMT cleavage plane are also shown.

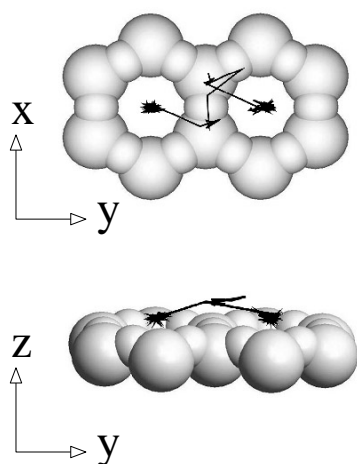


**Figure 5.** One representative  $\text{Li}^+$  jump in relation to the montmorillonite surface ( $T = 373$  K).

To quantify the above discussion on the mechanisms of ionic transport, we analyzed the correlations between the  $\text{Li}^+$  motion and the segmental dynamics of proximal polymer (Tables 1 and 2). Displacement of a  $\text{Li}^+$  ion greater than the mean distance between neighboring “trapping” sites (0.14 nm in the bulk and 0.35 nm in the intercalated systems) between successive saved system configurations is defined as a  $\text{Li}^+$  jump. For each of these jumps, all adjacent PEO moieties were checked on whether they undergo any of the following motions: trans-gauche isomerization, dihedral rocking (i.e., a change in the dihedral angle less than  $2\pi/3$ ), and/or translation of the EO carbon or oxygen atoms (over a distance larger than their atomic radius). Where such

segmental PEO motions take place just before the  $\text{Li}^+$  jump (within the same time scale as the jump occurs), we regard it as a correlation [Tables 1 and 2], whereas if no such segmental change takes place prior to a  $\text{Li}^+$  jump, we count it as an “uncorrelated  $\text{Li}^+$  motion”. Although the above definitions seem to be given on an ad hoc basis, the goal here is to establish whether PEO segmental motions mediate  $\text{Li}^+$  movement in their immediate vicinity and, if so, to further quantify this effect for each of these PEO segmental changes.

In the bulk systems, and for the lower temperatures, the lithium motion is highly correlated to the PEO dihedral dynamics (trans-gauche isomerization and dihedral rocking, table 1). This strong correlation, coupled with the slow EO dynamics, gives rise to the prolonged “trapping” of the lithiums and a “hopping”  $\text{Li}^+$  motion as seen in Figure 3 (e.g., at 323 K). As the temperature is raised, the  $\text{Li}^+$  motion still remains correlated to the PEO segmental dynamics, although the magnitude becomes now somewhat smaller (which is to be expected since now the  $\text{Li}^+$  coordinates less to the neighboring EO moieties). This weaker correlation is now manifested as the almost random, diffusive  $\text{Li}^+$  motion seen at 423 K in Figure 3. Throughout the temperature range,  $\text{Li}^+$  ion jumps are correlated to the ethylene oxide segmental motions, which is only natural as  $\text{Li}^+$  has to move within the bulk polymer.

In contrast, for the nanoconfined system, there exists a weaker correlation between  $\text{Li}^+$  jumps and adjacent EO dihedral dynamics throughout all temperatures [Table 2]. This weaker correlation is indicative of the  $\text{Li}^+$  coordination with the confining surfaces and reflects also in the nature of the  $\text{Li}^+$  transport mechanism on top of the walls (which remains the same over the entire temperature range). Still the PEO mediates the  $\text{Li}^+$

**Table 1. Correlation of Li<sup>+</sup> Motion (Jumps) with Segmental Changes in Bulk PEO (8 Li<sup>+</sup> over 2 ns)**

<i>T</i> (K)	Li <sup>+</sup> jumps		Li <sup>+</sup> jumps correlated to EO motions [ <i>L</i> /Li ns]				correlated fraction of Li <sup>+</sup> jumps
	total	/ <i>L</i> ns	trans-gauche isomerization	dihedral rocking	C and O motion	uncorrelated jumps	
273 (6 ns)	12	0.25	0.10	0.15	0.00	0.00	1.00
298 (4 ns)	9	0.28	0.09	0.19	0.00	0.00	1.00
323	17	1.06	0.31	0.62	0.13	0.00	1.00
373	126	7.88	1.56	6.19	0.13	0.00	0.98
398	221	13.81	1.38	9.89	0.94	1.60	0.82
423	342	21.38	1.50	13.75	5.00	1.13	0.71

**Table 2. Correlation of Li<sup>+</sup> Motion (Jumps) with Segmental Changes in the Confined Systems (42 Li<sup>+</sup> over 5 ns)**

<i>T</i> (K)	Li <sup>+</sup> jumps		Li <sup>+</sup> jumps correlated to EO motions [ <i>L</i> /Li ns]				correlated fraction of Li <sup>+</sup> jumps
	total	/ <i>L</i> ns	trans-gauche isomerization	dihedral rocking	C and O motion	uncorrelated jumps	
273	58	0.28	0.15	0.06	0.00	0.07	0.75
323	89	0.42	0.22	0.07	0.00	0.13	0.69
373	102	0.49	0.31	0.07	0.00	0.10	0.78
423	200	0.95	0.52	0.12	0.00	0.31	0.67

motion (at an almost *T*-independent 70% level), because the lithium moves from one wall “pocket” to another by moving through the PEO molecules present in interlayer. To further verify this inference, we carried out control tests where we (a) measured the inverse correlation, i.e., to what extent the same EO dynamics do not result in lithium jumps, in which case we found it to be a very small number, and (b) froze the EO dihedral dynamics in the confined system, in which case all Li<sup>+</sup> motion was arrested.

From Figure 4 and the above discussion, it becomes obvious that the Li<sup>+</sup> mobility is determined by the *balance* of the Li<sup>+</sup> interactions with the PEO and the MMT and the PEO segmental dynamics. Namely, a competitive coordination of the Li<sup>+</sup> by the negatively charged MMT and the PEO results in an *excess* interaction energy that “binds” the cations on the MMT surface. This excess energy is the main component of the activation energy for Li<sup>+</sup> diffusion;<sup>20</sup> on the basis of the above molecular picture, one can envision system modifications that would result in higher Li<sup>+</sup> diffusivities and, thus, also higher conductivities. For example, if the MMT/Li<sup>+</sup> interactions are better balanced by the polymer/Li<sup>+</sup> interactions, then the Li<sup>+</sup> diffusivity should increase considerably. This can be achieved by either reducing the MMT layer charge<sup>21</sup> or by selecting a polymer that interacts as strongly with Li<sup>+</sup> as MMT does. In both of these cases, there will be a sensitive balance between parameters which control the system conductivity, and these parameters should be optimized, namely, a reduced MMT layer charge will result in an increased Li<sup>+</sup> mobility but will also reduce the number of carriers. Along the same lines, small increases in the polymer/

Li<sup>+</sup> interactions will promote the Li<sup>+</sup> unpinning from the MMT surfaces and thus increase the carrier mobility; however, much stronger interactions could potentially move the carriers to the center of the polymer film, and then the molecular details would be completely different.

## Conclusions

Li<sup>+</sup> dynamics as well as correlations between Li<sup>+</sup> motion and proximal ethylene-oxide dynamics have been investigated in bulk and nanoscopically confined systems. Simulations have revealed a single hopping mechanism for Li<sup>+</sup> motion over a wide temperature range in intercalated PEO, whereas in the same *T* range for bulk PEO, there exist two distinct mechanisms: a hopping motion at low temperatures and a random, Brownian-like behavior at higher temperatures. Closer observation of the Li<sup>+</sup> trajectories in the intercalated systems shows that the cationic motion is dictated by the competitive coordination of the Li<sup>+</sup> to the MMT surfaces and the PEO. Furthermore, a strong correlation between the motion of Li<sup>+</sup> and PEO segmental dynamics in these confined systems supports that PEO dynamics in the interlayer gallery influence the Li<sup>+</sup> motion on top of the confining wall. These molecular mechanisms of motion are also reflected in the MD diffusivities, which capture the trends, temperature dependence, of experimentally measured ionic conductivities.<sup>7</sup>

**Acknowledgment.** This work was supported through the Penn State MRSEC (NSF/DMR 0080019), and for V.K. support through NIST/BFRL (DoC Grant 60NANB1D0066) is also thankfully acknowledged.

**Supporting Information Available:** Force field parameters for the MD simulations (PDF). This material is available free of charge via the Internet at <http://pubs.acs.org>.

CM011275W

(19) Shi, J.; Vincent, C. A. *Solid State Ionics* **1993**, *60*, 11.

(20) The fact that our simulated values of *D* follow well the experimental behaviour (Figure 2) indicates that the force fields used reproduce faithfully the interactions of the real systems.

(21) Madejova, J.; Bujdak, J.; Gates, W. P.; Komadel, P.; *Clay Miner.* **1996**, *31*, 233. Theng, B. K. G.; Hayashi, S.; Soma, M.; Seyama, H. *Clays Clay Miner.* **1997**, *45*, 718. Alvero, R.; Alba, M. D.; Castro, M. A.; Trillo, J. M. *J. Phys. Chem.* **1994**, *98*, 7848.